Efficient Simulation of Mobile-To-Mobile Rayleigh Fading using Gaussian Quadrature

Kevin C. Borries, Daniel D. Stancil
Dept. of Electrical and Computer Engineering
Carnegie Mellon University
Pittsburgh, PA 15213 USA

Abstract—The Gaussian quadrature rules (GQRs) are used to construct a wireless fading simulator based on the popular sum of sinusoids (SoS) method. The general statistics of the proposed simulator are given. This simulator is also shown to perform well for important design parameters. An extension of the GQRs is employed to build uncorrelated simulators, which are important in frequency selective and MIMO simulators. These simulation techniques are then applied to the Mobile-to-Mobile (MtM) spectrum and are compared with the best known SoS techniques for the MtM spectrum. Although the proposed method is more complex, the efficiency and accuracy are significantly better than the previously proposed methods.

Keywords-Fading channel simulator; sum-of-sinusoids; mobile-to-mobile channel.

I. Introduction

Wireless channel simulators play an important role in the research and development of modern communication systems. One key requirement of a wireless simulator is the generation of a fading channel caused by Doppler spread. Not only is this fading a dominate feature in narrowband channels, but wideband frequency selective channels are often simulated using an array of uncorrelated fading waveform generators [1, ch. 7].

Many different techniques have been developed to build fading waveforms. These techniques can be divided into two main categories: the filter method [2, 3], and the sum of sinusoids (SoS) method. The SoS simulator has received considerable attention recently, because this method balances accuracy with flexibility and simulation speed [1, ch. 8].

The SoS simulator adds sinusoids with prescribed frequencies and amplitudes, but random phases [4]. This simulator is very accurate for various Doppler spectra and can generate fading samples as needed rather then in large blocks as in [2]. These properties make the SoS simulator very attractive for applications that require fast and flexible computations such as a real-time simulator. The frequencies and amplitudes of the SoS simulator can be computed either deterministically or statistically. The deterministic method gives excellent accuracy, but only a limited number of uncorrelated simulators can be built. The statistical method can generate a large number of uncorrelated simulators, but there may be a large variation of accuracy due to the randomness of the parameters [5].

This research is sponsored by the National Science Foundation

Many techniques have been developed to generate parameter values for deterministic [4] and statistical [6, 7] SoS. These methods are usually specific to the shape of the Doppler spectrum and have typically been applied to the mobile-to-stationary channel. The shape of the mobile-to-mobile (MtM) Doppler spectrum is more complex, and only recently have statistically valid SoS techniques been presented to simulate the MtM Doppler spread [8].

Gaussian Quadrature Rules (GQRs) can be applied to generate SoS parameters for a variety of band-limited spectra [9, 10]. Although the GQRs have been applied to a number of practical spectra, the rules have not yet been developed for more complex spectra such as the MtM spectrum. These rules are not random, therefore the resulting SoS simulator is deterministic. A variation on the GQRs, Patterson's quadrature formulas (PQFs), allows for randomness in the SoS parameters [11] which leads to a statistical SoS simulator.

The paper is organized as follows. Section II gives the theoretical background of the SoS with GQRs and PQFs. Section III describes the procedure for applying GQRs and PQFs to the MtM spectrum. Section IV compares the GQRs and PQFs methods to the best known SoS methods for the MtM spectrum.

II. THEORETICAL BACKGROUND

A. SoS Simulator Statistics

The complex signal produced by the SoS simulator g(t) can be represented by the following functions:

$$g_{i}(t) = \sum_{n=1}^{N} c_{i,n} \cos(2\pi f_{i,n} t + \theta_{i,n}),$$
 (1)

$$g_{q}(t) = \sum_{n=1}^{N} c_{q,n} \cos(2\pi f_{q,n} t + \theta_{q,n}),$$
 (2)

$$g(t) = g_i(t) + jg_q(t).$$
(3)

The amplitudes $c_{i/q,n}$ and frequencies $f_{i/q,n}$ are generated by the chosen SoS method and the phases $\theta_{i/q,n}$ are independent and uniformly distributed from 0 to 2π ; i.e. $\theta_{i/q,n} \sim U[0, 2\pi)$. The phases are random so that $g_i(t)$ and $g_q(t)$ will be close to a Gaussian distribution by the central limit theorem, assuming N > 6 [4]. The resulting probability distribution function (PDF) of g(t) will be close to the theoretical definition for Rayleigh fading. Assuming all frequencies are unique, the principle of orthogonal cosines can be used to find the autocorrelations:

$$R_{g_i g_i}(\tau) = \sum_{n=1}^{N} c_{i,n}^2 \cos(2\pi f_{i,n} \tau) / 2,$$
 (4)

$$R_{g_q g_q}(\tau) = \sum_{n=1}^{N} c_{q,n}^2 \cos(2\pi f_{q,n} \tau) / 2,$$
 (5)

$$R_{gg}(\tau) = R_{g_0g_0}(\tau) + R_{g_0g_0}(\tau). \tag{6}$$

The SoS amplitudes and frequencies should be chosen so that the SoS autocorrelations (4-6) match the desired autocorrelations as closely as possible. Most simulation tests require that the simulated autocorrelation closely matches the theoretical autocorrelation up to a maximum delay of τ_{max} for a given maximum autocorrelation error. At delays larger than τ_{max} , the autocorrelation of the channel is not relevant to the communication process under test; e.g., τ_{max} could be the packet length.

A second important parameter in evaluating simulators is the second derivative of the autocorrelation at $\tau = 0$,

$$\beta = -\ddot{R}_{gg}(0). \tag{7}$$

This parameter is called the spread factor because it is related to the rms Doppler spread [4]. The spread factor directly impacts the level crossing rate and the average fade duration of the resulting simulation. The spread factor for the SoS is given by [4]

$$\beta_{SOS} = \pi^2 \left[\sum_{n=1}^{N} (c_{i,n} f_{i,n})^2 + (c_{q,n} f_{q,n})^2 \right].$$
 (8)

If β is the desired spread factor, then the performance of the SoS simulation can be evaluated with the relative difference,

$$\beta_{diff} = |\beta - \beta_{SoS}| / \beta. \tag{9}$$

For statistical SoS simulators the autocorrelations and spread factor are random variables and do not always match the ideal case for a given trial. Therefore, another performance measure is needed to determine how far on average the SoS statistics may deviate from the ideal. This measure is the variance of the autocorrelation or the mean squared distance from the ideal autocorrelation $R_i(\tau)$,

$$\operatorname{var}[R(\tau)] = \operatorname{E}\left(\left|R_{gg}(\tau) - R_{t}(\tau)\right|^{2}\right). \tag{10}$$

B. Gaussian Quadrature Properties

Gaussian Quadrature is a classic technique for high precision numeric integration. A foundational problem in numeric integration is how to approximate an integral as a sum of samples of the integrand at nodes x_n each times a corresponding weight w_n ; i.e.,

$$\int_{a}^{b} \omega(x) f(x) dx = \sum_{n=1}^{N} w_n f(x_n) + E.$$
(11)

A GQR is a set of weights and nodes that attempts to minimize the approximation error E for a weight function $\omega(x)$. The GQRs give the exact value of the integral of a polynomial fit of f(x) times $\omega(x)$. This fit is of the order 2N-1, where N is the

number of points in the summation. The beauty of the GQRs is that the weights and nodes do not depend on the function f(x) but only on the chosen weight function and number of nodes. The limits of integration will only define a linear scaling of the weights and nodes.

A GQR is based on a set of orthogonal polynomials. The integration interval and weight function over which the polynomials are orthogonal give the limits and $\omega(x)$ for the GQR. The roots of the Nth polynomial give the nodes of the Nth point GQR. An explanation of the theory behind the GQRs can be found in [12].

A proper choice of $\omega(x)$ can greatly improve the accuracy of the GQRs. The simplest case is if the integrand f(x) is approximated well by a polynomial. Then $\omega(x) = 1$ will be sufficient, and the corresponding Gauss-Legendre rules can be used. If a polynomial fit does not suit f(x) but will work well for $f(x)/\omega(x)$, then the GQRs can be written

$$\int_{a}^{b} \omega(x) f(x) / \omega(x) dx = \sum_{n=1}^{N} w_n f(x_n) / \omega(x_n) + E.$$
 (12)

The GQRs can be applied to the SoS parameter generation by observing that the autocorrelation function is the inverse Fourier transform (IFT) of the power spectral density (PSD), represented as S(f). Assuming that the Doppler spectrum is band-limited and symmetric, the autocorrelation is

$$R_{t}(\tau) = \int_{0}^{f_{\text{max}}} 2S(f)\cos(2\pi f \tau)df. \tag{13}$$

The band-limited assumption is true for all real world Doppler spectra. Asymmetrical spectra can be simulated by inducing a correlation between $g_i(t)$ and $g_q(t)$ [4 ch. 6]. Applying GQRs to the IFT in (13) gives

$$R_{t}(\tau) = \sum_{n=1}^{N} 2w_{n} S(f_{n}) \cos(2\pi f_{n} \tau) / \omega(f_{n}) + E.$$
 (14)

This representation of the autocorrelation is in the same form as the autocorrelations given in (4-6). Comparing (14) with (4) and (5) reveals that the SoS frequencies $f_{i/q,n}$ are the nodes f_n of the GQRs from (14) and the amplitudes are found to be

$$c_{i,n} = \sqrt{w_n S(f_n)/\omega(f_n)}. \tag{15}$$

The GQRs are only as good as the polynomial fit on $f(x)/\omega(x)$. In (14), $f(x)/\omega(x)$ contains a cosine term which has a good polynomial fit only for low frequencies. The GQRs will be a good approximation up to a certain τ_{max} . When τ is zero, the cosine term is one. Consequently, if $S(f)/\omega(f)$ can be closely approximated by a polynomial as $\tau \to 0$, the GQRs produce the exact autocorrelation and the simulation reproduces the ideal spread factor.

The GQRs can be used to generate parameters for either $g_i(t)$ or $g_q(t)$, but not both. If the spectra for the I and Q components are the same, then the GQRs will give the same parameters which contradicts the assumption of uncorrelated quadrature components. A simple way to fix this problem is to let the Q component have one more term than the I component

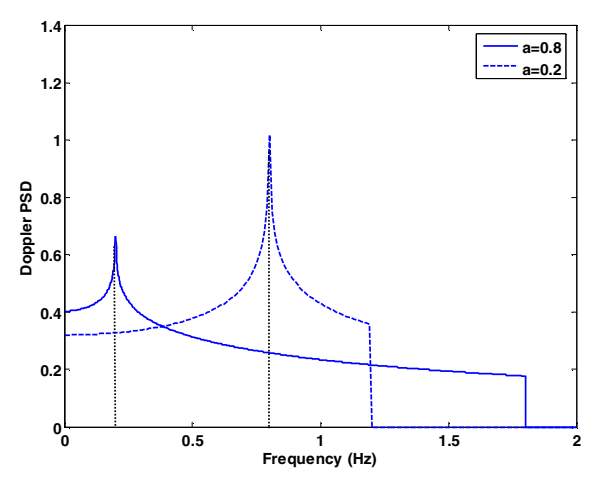


Fig. 1. Doppler spectrum for $f_1 = 1$ Hz. The vertical lines mark the singularity. To the left of the singularity is the middle-section; to the right is the end-section. The full spectrum is symmetric about zero.

[4]. The GQRs are interpolatory in nature; consequently the nodes for a GQR of order N+1 will all be different from the nodes of a GQR of order N. This technique will ensure that the I and Q components are uncorrelated, but can only produce a limited number of practical uncorrelated simulators. This problem can be solved though the calculation of PQFs.

PQFs address the following question: given P preassigned nodes, what are the M nodes and P+M weights that optimize the approximation in (11)? PQFs give the optimum weights and added nodes with respect to a chosen GQR. The resulting precision is the same polynomial fit of f(x) as the GQRs but with an order of at least 2M+P-1 [11]. Different preassigned nodes will result in different calculated nodes. If only one preassigned node is used, the calculated nodes will all be unique from the set calculated from a different preassigned node, assuming that the two preassigned nodes are not members of each other's calculated nodes.

For the SoS application the nodes represent frequencies, and only one preassigned frequency is used to maximize precision. The preassigned frequency is chosen at random for each simulator, and PQFs are used to calculate the optimal set of amplitudes and frequencies. The calculated frequencies will be unique across all of the simulators, because each simulator uses a different preassigned frequency. Thus, the simulators will all be uncorrelated.

PQFs are based on the GQRs so the same performance is given by the SoS generated from PQF as from GQRs. Therefore, the spread factor should be ideal for any SoS generated from PQF, provided that $S(f)/\omega(f)$ is closely approximated by a polynomial. Also, the variance of the autocorrelation will be small, because the precision of the polynomial fit will always be the same.

One drawback with PQFs is that not all preassigned nodes result in calculated nodes that are real and within the range of the PSD. Typically, about 50-80% of the possible preassigned nodes will give valid results. This problem can be solved by finding the ranges of good preassigned nodes and then limiting the preassigned nodes to those ranges.

III. GQRS APPLIED TO THE MTM SPECTRUM

A. Properties of the MtM Spectrum

The MtM spectrum models the Doppler spread when both the transmitter and receiver are in motion. The PSD and autocorrelation are given by [13]¹

$$S(f) = \frac{\text{Re}[K[Q(f)]]}{\pi^2 \sqrt{a} f_1} \quad 1 \ge a > 0 \quad |f| < f_1(1+a), \tag{16}$$

$$R_{g,g,}(\tau) = R_{g,g_q}(\tau) = R_{gg}(\tau) = J_0(2\pi f_1 \tau) J_0(2\pi f_2 \tau),$$
 where

$$a = f_2 / f_1, \tag{18}$$

 f_1 and f_2 are the maximum mobile-to-stationary Doppler frequencies of the faster and slower antennas respectively, and

$$Q(f) = \sqrt{(1+a)^2 f_1^2 - f^2/(4af_1^2)}.$$
 (19)

The function $K[\cdot]$ represents the complete elliptic integral of the first kind and $J_0(\cdot)$ represents the zeroth-order Bessel function of the first kind. The cross-correlation between g_i and g_q is zero. The PSD for a=0.2 and a=0.8 is plotted in Fig. 1. When $|f| < f_1(1-a)$, Q(f) > 1 and the elliptic integral results in a complex number. If numerical support for complex elliptic integrals is not available, the identities in [14, p. 337] can be applied to transform the PSD into a form with all real elliptic integrals. The resulting PSD is

$$S(f) = K[1/Q(f)]/(\pi^2 \sqrt{a} f_1 Q(f)) |f| < f_1(1-a).$$
 (20)

The spread factor for the MtM spectrum is given by [15]

$$\beta = 2(\pi f_1(1+a))^2. \tag{21}$$

B. GOR MtM Simulator

The PSD for the MtM case contains singularities at $|f| = f_1(1-a)$. Since this PSD cannot be closely approximated with a polynomial, a GQR with $\omega(f) = 1$ will result in significant errors. The PSD approaches these singularities asymptotically on the order of a natural log approaching zero. Therefore, a weight function that is a natural log will eliminate the singularities. The log weight function is not a characteristic of any of the classical GQRs, but the weights and nodes of this GQR can be found by recursion with the method of modified moments given as an example in [12, p. 159]. Because the log function has only one singularity, the PSD in (16) must be split into two sections which we will call the end-section and the middle-section. The weight function of the end-section can be expressed as

$$GQ1 = -\int_0^1 \ln(2ax/\alpha)f(x)dx,$$
 (22)

and for the middle-section the weight function is given by

$$GQ2 = -\int_0^1 \ln((1-x)(1-a)/\alpha)f(x)dx,$$
 (23)

where α is a shaping parameter. These weight functions are designed to eliminate the singularity in each section as well as

¹ The reference does not include Re[] in the equation for the PSD, but it is clear from the proof that it should be included.

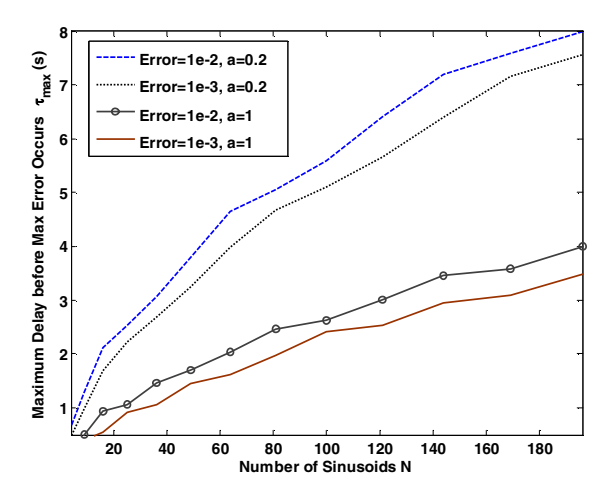


Fig.2. The number of sinusoids needed for a given τ_{max} and maximum error with the MMEDS method.

be in a convenient form for solving the quadrature rules.

The value of α is critical to the accuracy of the GQR. The derivative of the scaled version of the MtM PDF over the weight functions in (22, 23) is infinite at the singularity except for a particular value of α . By extending the limit in [14 p. 591] to

$$\lim_{f \to 0} \left(K \left\lceil \sqrt{1 - (f/\beta)^2} \right\rceil + \ln(f) \right) = \ln(4\beta), \tag{24}$$

and applying this limit to the singularity of the derivative, the required values of α can be shown to be

$$\alpha = \begin{bmatrix} 32f_1 a/(1-a) & a < 1 \\ 8f_1 & a = 1 \end{bmatrix}$$
 (25)

With these values of α and the weight functions given in (22, 23), the resulting functions $S(f)/\omega(f)$ will be continuous, and a reasonable good approximation can be obtained with a polynomial fit. However, a new GQR must be calculated for each value of a.

The GQRs from (22, 23) require that the spectrum be split into two segments. The total number of sinusoids used, N, should be split between the two quadrature rules to maximize the parameters given in Section I. The ratio of nodes in the middle-section to the total number of nodes we define to be the splitting factor, F. The optimum splitting factor is a function of a and is generally not dependant of the total number of sinusoids N for N > 14. The optimum values of F were found numerically by minimizing the error in the spread factor using (21) and (8) for N = 50 and 185 linearly-spaced values of a in the range [0.04, 0.96]. The resulting curve is a close fit for the polynomial

$$F = 4.76r^5 - 12.2r^4 + 12.4r^3 - 6.20r^2 + 2.03r + 0.0917,$$
 (26) where.

$$r = (1 - a)/(1 + a). (27)$$

If F*N is not an integer, then this number is rounded to the nearest integer. There are numerical problems in the algorithm if there is only one point in a section. Therefore, if N-F*N or

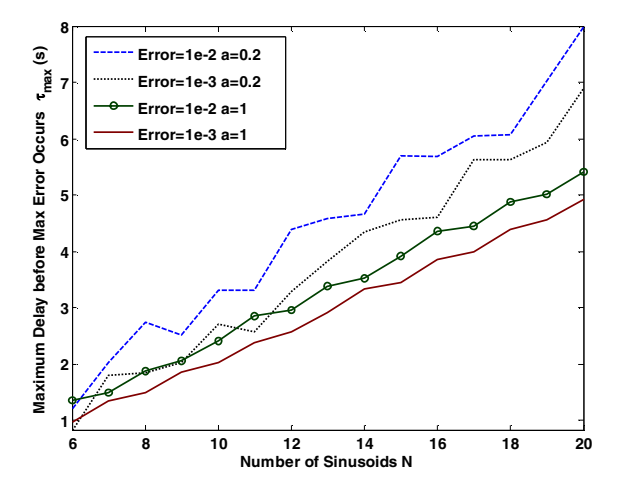


Fig.3. The number of sinusoids needed for a given τ_{max} and maximum error with the GQR method.

 F^*N is one, then another point is added to the single point section.

PQFs can be applied to this spectrum to give uncorrelated simulators. PQFs require a recursion relation for the coefficients of the orthogonal polynomial used to generate the GQR. The benefit of generating the GQRs in (22, 23) with the method of modified moments, is that this recursion relation is calculated in the procedure. The procedure is as follows. First the weighting functions for (22, 23) are found. Then the method of modified moments is applied to find the recursion relation for each GQR. Next, a preassigned frequency is selected at random for each segment. The optimal amplitudes and frequencies for each segment are calculated with PQFs according to the preassigned frequency. Lastly, the amplitudes are scaled according to samples of the spectrum at the calculated frequencies. The last two steps are repeated with different preassigned frequencies until the desired number of uncorrelated simulators is achieved.

IV. PERFORMANCE OF GQR TECHNIQUES

A. Deterministic Models

The GQR simulator has been defined for the MtM channel in the previous section. This SoS simulator is now compared with the modified method of exact Doppler spread (MMEDS) for MtM fading [5]. The equations for the MMEDS simulator are not given here because of space constraints, but a detailed description of the method can be found in [5].

The performance of the two simulators is measured by calculating τ_{max} across a range of values of N having different maximum errors and values of a, with $f_1 = 1$ Hz and a sampling frequency of $f_s = 1$ kHz. The test was performed on only the I component, because the autocorrelation is the same for both components. The results are shown in Figs. 2, 3. The τ_{max} plots show that the GQR method requires significantly fewer sinusoids than MMEDS for the same τ_{max} . Therefore, the GQR method is a much faster simulator with the same accuracy. However, the SoS parameters are much easier to compute for the MMEDS case which may make it more practical for shorter simulations.

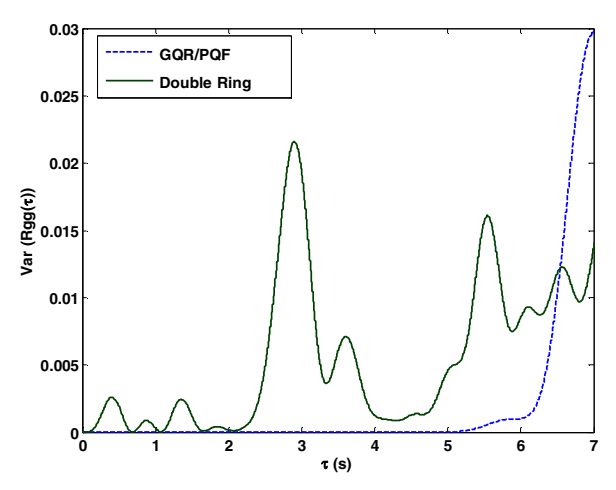


Fig.4. Variance of the autocorrelation of the statistical SoS.

The spread factor for the MMEDS will always be exact. This is not the case for the GQR method. Nevertheless, the relative difference between the theoretical and the ideal spread factors (9) will be very small; e.g., the maximum relative difference in spread error for N = 20 is about $4*10^{-7}$, with a = [0.05, 0.95].

B. Statistical Models

The double ring model is the best known statistical MtM fading simulator in terms of autocorrelation variance [5]. The details of the double ring model, as well as the equations for the autocorrelations, are given in [5]. This model is compared with the GQRs with PQFs, or GQR/PQF, when the preassigned frequency is independently drawn from $f_p \sim U[0, f_{max})$.

The statistical models were tested by calculating the variance in the autocorrelation of the complex signal as defined in (10). The variances were computed over 10^4 trials, with $f_1 = 1$ Hz and $f_s = 1$ kHz. Fig. 4 compares the variances of the GQR/PQF model to the double ring model; both with 16 sinusoids and a = 0.2. The results in Fig. 4 clearly show that the GQR/PQF method gives much lower variance than the double ring model in the important region where τ is low. Although the double ring model performs better for larger τ , for practical tests the statistics for longer delays are much less important than those for short delays. However, parameters for the double ring model are very easy to compute, so this simulator may be faster for very short simulations with moderate accuracy requirements.

Another benefit for the GQR/PQF model is that spread error will consistently be low. This is not the case with the double ring simulator. Therefore, the level crossing rate and average fade duration will be consistently much more accurate with the GQR/PQF model. To illustrate this point Table I gives the variance of the spread factor for the same simulations in Fig. 4 for various values of *a*.

V. CONCLUSION

This paper has shown that the GQRs and PQFs can be used to develop new deterministic and uncorrelated statistical SoS fading simulators. These techniques were applied to the MtM

TABLE I VARIANCE OF SPREAD ERROR

а	Var(β) GQR/PQF	$Var((\beta)$ Double Ring
0.2	1.54*10 ⁻¹⁶	5.49*10 ⁻³
0.5	$6.30*10^{-14}$	$3.47*10^{-2}$
0.8	$8.50*10^{-13}$	8.86*10 ⁻²
1	5.94*10-9	0.138

channel and compared to current MtM simulators. The parameters for the SoS are easier to calculate with the current simulators. However, the GQR/PQF simulators perform much better in terms of matching the autocorrelation with fewer sinusoids. The deterministic simulator for GQR does slightly worse than the MMEDS in terms of the spread factor, but the error is small enough in the GQR model that they are both practically ideal. The GQR/PQF is a significant improvement over the best current statistical MtM simulator in terms of the spread factor.

REFERENCES

- [1] M Pätzold, Mobile Fading Channels. West Sussex, UK: Wiley, 2002.
- [2] M. Kahrs and C. Zimmer, "Digital signal processing in a real-time propagation simulator," *IEEE Trans. Instrum. Meas.*, vol. 55, no. 1, pp. 197-205, Feb. 2006.
- [3] D. J. Young and N. C. Beaulieu, "The generation of correlated Rayleigh random variates by inverse discrete Fourier transform," *IEEE Trans. Commun.*, vol. 48, no. 7, pp. 1114-1127, July 2000.
- [4] M. Pätzold, U. Killat, F. Laue, and Y. Li, "On the statistical properties of deterministic simulation models for mobile fading channels," *IEEE Trans. Veh. Technol.*, vol. 47, no. 1, pp. 254-269, 1998.
- [5] C. S. Patel, G. L. Stuber, and T. G. Pratt, "Comparative analysis of statistical models for the simulation of Rayleigh faded cellular channels," *IEEE Trans. Commun.*, vol. 53, no. 6, pp. 1017-1026, Jun. 2005
- [6] Y. R. Zheng and C. Xiao, "Improved models for the generation of multiple uncorrelated Rayleigh fading waveforms," *IEEE Commun. Lett.*, vol. 6, no. 6, pp. 256-258, Jun. 2002.
- [7] Y. X. Li and X. Huang, "The simulation of independent Rayleigh faders," *IEEE Trans. Commun.*, vol. 50, pp. 1503-1514, Sept. 2002.
- [8] C. S. Patel, G. L. Stüber and T. G. Pratt, "Simulation of Rayleigh-faded mobile-to-mobile communication channels," *IEEE Trans. Commun.*, vol. 53, pp. 1876-1854, no. 11, Nov. 2005.
- [9] S. Y. Kwan and N. M. Shehadeh, "Analysis of Incoherent Frequency-Shift Keyed Systems," *IEEE Trans. Commun.*, vol. 23, no. 11, pp. 1331-1339, Nov. 1975.
- [10] D. R. Hummels and F. W. Ratcliffe, "Calculation of error probability for MSK and OQPSK systems operating in a fading multipath environment," *IEEE Trans. Veh. Technol.*, vol. 30, no. 3, pp. 112-120, Aug. 1981.
- [11] T. N. L. Patterson, "An algorithm for generating interpolatory quadrature rules of the highest degree of precision with preassigned nodes for general weight functions," ACM Trans. Mathematical Software, vol. 15, no. 2, pp. 123-136, June 1989.
- [12] W. H. Press et al., Numeric Recipes in C: The Art of Scientific Computing. Cambridge: Cambridge University Press, 1992.
- [13] A. S. Akki and F. Haber, "A statistical model for mobile-to-mobile land communication channel," *IEEE Trans. Veh. Technol.*, vol. VT-35, no. 1, pp. 2-7, Feb. 1986.
- [14] M. Abramowitz and I. A. Stegun, Handbook of Mathematical Functions with Formulas, Graphs, and Mathematical Tables. Washington D.C.: U. S. Govt. Print. Off., 1972.
- [15] A. S. Akki, "Statistical properties of mobile-to-mobile land communication channels," *IEEE Trans. Veh. Technol.*, vol. 43, no. 4, pp. 826-831, Nov. 1994.